Electrical characterizations of a controllable field emission triode based on low temperature synthesized ZnO nanowires

2006 Nanotechnology 17 83

(http://iopscience.iop.org/0957-4484/17/1/014)

INSTITUTE OF PHYSICS PUBLISHING NANOTECHNOLOGY
Nanotechnology **17** (2006) 83–88 doi:10.1088/0957-4484/17/1/014

Electrical characterizations of a controllable field emission triode based on low temperature synthesized ZnO nanowires

Chia Ying Lee[1], Tseung Yuen Tseng[1,2,4], Seu Yi Li[3] and Pang Lin[3]

[1] Department of Electronics Engineering and Institute of Electronics, National Chiao Tung University, Hsinchu 300, Taiwan
[2] Department of Materials and Mineral Resources Engineering, National Taipei University of Technology, Taipei 106, Taiwan
[3] Institute of Materials Science and Engineering, National Chiao Tung University, Hsinchu 300, Taiwan

E-mail: tseng@cc.nctu.edu.tw

Received 26 August 2005
Published 1 December 2005
Online at stacks.iop.org/Nano/17/83

Abstract
Fabrication and field emission properties of a ZnO nanowire (NW) triode were investigated in this study. The ZnO NWs have a single-crystalline wurtzite structure, ∼50 nm diameter and 3.4×10^{10} cm^{-2} number density. The ZnO NW triode shows good and controllable emission properties with the turn-on anode electric field (at a current density of 1 μA cm^{-2}), threshold anode electric field (at a current density of 1 mA cm^{-2}) and field enhancement factor of 1.6, 2.1 V μm^{-1} and 3340, respectively. The ZnO NW triode exhibits transistor characteristics with a gate leakage region, linear region and saturation region. Furthermore, the controllable field emission performance of the ZnO NW triode can be enhanced by illumination and argon ion bombardment. A low temperature Si-based microelectronic compatible fabrication process was provided for successfully making ZnO NW based triodes with good field emission properties.

1. Introduction

Current trends in nanotechnology and nanomaterials play an important role in the potential applications of photonic, electro-optical and electronic devices because of their unique physical and chemical properties [1–4]. In particular, exploration of the materials for flat panel displays has been a hot topic for the last few decades. High aspect ratio one-dimensional (1D) nanostructures, such as nanotubes, nanowires and nanobelts, have been extensively studied with a view to use in vacuum microelectronic devices, including field emission displays (FEDs), electron sources, microwave devices and high power rf amplifiers, because of the advantage of the low turn-on electric field and high electron emission efficiency [3–5]. The main advantages for the FED are a large area display, high uniformity, high productivity, high brightness, low cost, low power consumption and reliability. From this point of view, triode-type FED devices with low driving voltage, high resolution and controllable electron emission characteristics are candidates for constituting a new generation of FED devices.

ZnO, with its wide band gap (3.4 eV) and large exciton binding energy (60 meV), has attracted much attention since possible applications in phosphors, transparent conducting films for solar cells, ultra-violet (UV) laser devices and flat panel displays were suggested [6–9]. Recently, ZnO NW emitters have been reported to exhibit good emission properties with high stability, low threshold electric field, high emission current density, good emission stability and

[4] Author to whom any correspondence should be addressed.

durability [9, 13]. The ZnO NWs have been synthesized by various procedures [10–12]; however, the main challenge in fabricating the NW based FED devices is the high synthesis temperature which retards the integration processes for FED device structures. A hydrothermal method would offer a superior route for FED fabrication because of the catalyst-free growth, low cost, low reaction temperature, large area and uniform production, environment friendliness and process compatibility with VLSI.

Although field emission triodes based on CNTs and diamond films have been developed [14, 15], devices based on ZnO NWs are seldom discussed. In this article, a hydrothermal method is adopted to fabricate ZnO NWs in a field emission triode device at 75 °C, and the controllable field emission characteristics are investigated.

2. Experiments

A field emission triode based on ZnO NWs was fabricated on a p-type Si(100) substrate. Figure 1(a) illustrates the fabrication flow of a ZnO NW triode field emission array. The process began with plasma-enhanced chemical vapour deposition (PECVD) of SiO_2 on the Si substrate, followed by electron beam evaporator deposition of gate electrodes, made of Al. The thicknesses of the insulating oxide and the gate metal were 500 and 100 nm, respectively. The emitter regions were defined by a standard photolithography and wet etching process. An ultrathin ZnO film (∼70 Å) was deposited on the substrate by rf sputtering (13.56 MHz) under Ar sputtering gas at a base pressure of 20 mTorr; this was used as a seeding layer to prepare well-aligned ZnO NWs by the hydrothermal method. Then, the photoresistance (PR) layer was stripped, and the unwanted seeding above the metal gate layer was lifted off. Last, the substrate was put into an aqueous solution (Milli-Q, 18.2 MΩ cm) of zinc nitrate hexahydrate ($Zn(NO_3)_2{\cdot}6H_2O$, 0.01 M) and diethylenetriamine (HMTA, $C_6H_{12}N_4$, 0.01 M) in a sealed vessel at 75 °C for 30 min. A more detailed description of the hydrothermal method was given in [1]. When the NWs were grown hydrothermally on the substrate, the fabrication of the triode device was completed.

The crystal structure of the ZnO NWs was examined by means of x-ray diffraction (XRD, MAC Science, MXP18, Japan). The surface morphologies of the NWs were observed by field emission scanning electron microscopy (FE-SEM, Hitachi S-4700I, Japan) and high resolution transmission electron microscopy (HR-TEM, Philips Tecani-20). The test scheme corresponding to the field emission measurement is illustrated in figure 1(b). The measurement was carried out in a vacuum chamber (base pressure of 1×10^{-6} Torr) equipped with a valve through which Ar gas flows in, to adjust the measuring pressure. A Keithley 237 current–voltage analyser was used for measuring the field emission characteristics and a power supply was adopted for the control of the gate bias (V_g). A copper electrode probe that serves as an anode with the tip diameter of 500 μm was placed at a distance of 500 μm from the tips of the NWs. The electrode distance was adjusted using a precision screwmeter with an accuracy of ±0.1 μm.

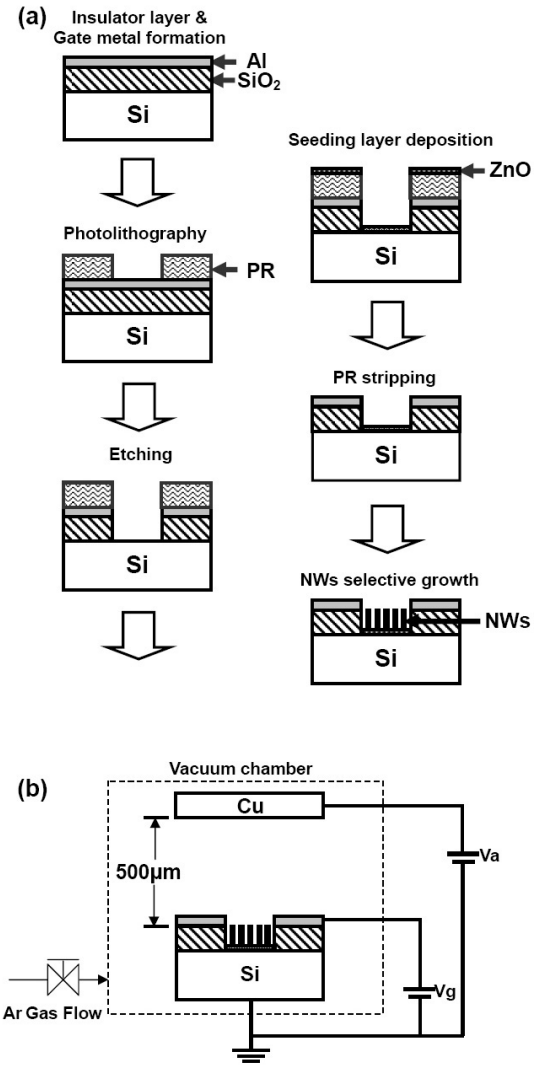

Figure 1. (a) Schematic description of fabrication processes for the field emission triode. (b) Test system for the triode mode.

3. Results and discussion

A low magnification SEM image of the fabricated 2 × 2 ZnO based triode array is shown in the inset of figure 2, indicating that the cathode active region is a square opening of $100 \times 100\ \mu m^2$, and the distance between the two active regions is 500 μm. The ZnO NWs are successfully and selectively grown inside the gate hole with ZnO seeding areas, but no NWs and other impurities are grown on the gate regions. Figure 2 is an enlarged image of the triode device, in which there are well-aligned ZnO NWs with an average diameter of 50 nm and a number density of 3.4×10^{10} cm^{-2}. These ZnO NWs are randomly oriented, and uniformly and selectively grown on ZnO seeding layers inside the cathode active regions.

Figure 3(a) shows the XRD pattern of the ZnO NWs of the field emission triode. The peaks at 33.08° and 38.5° in the XRD patterns are caused by the Si substrate and Al metal gate, respectively. The crystal structure of these ZnO NWs is wurtzite and no other phases appear. The lattice constants calculated from the XRD patterns of hydrothermally

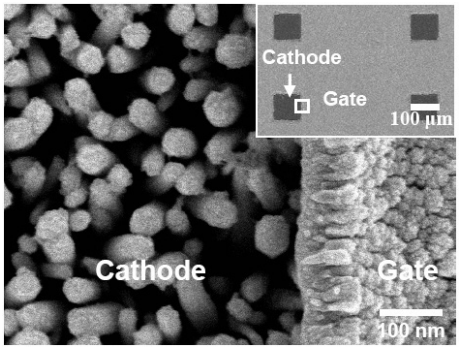

Figure 2. Typical FE-SEM micrographs near the gate edge of a ZnO NW triode; the inset shows the 4 × 4 array triode with ZnO NWs grown inside gate holes.

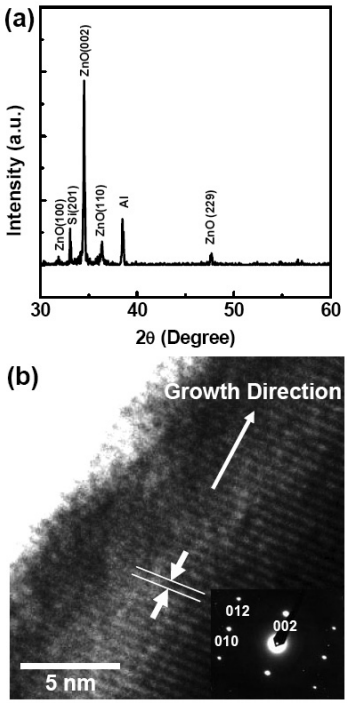

Figure 3. (a) XRD pattern of the ZnO NW triode. (b) HRTEM micrograph of ZnO NWs; the inset shows the corresponding SAED of the NWs.

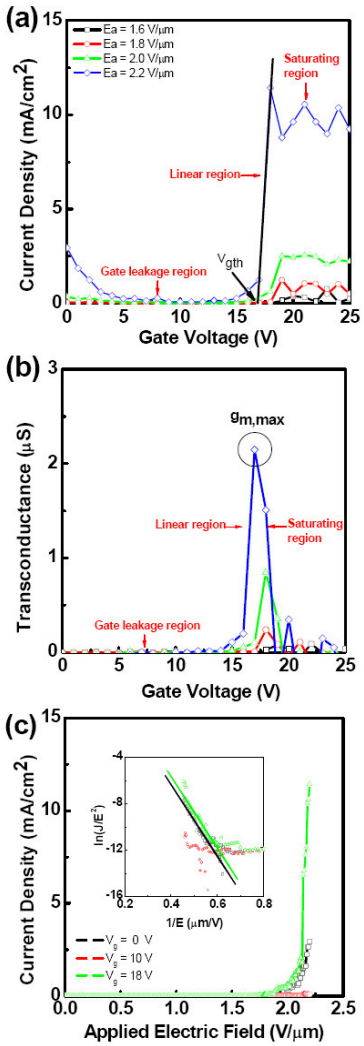

Figure 4. (a) Field emission current density versus gate voltage (J–V_g) curves under the various applied electric fields. (b) Relation of transconductance versus gate voltage for the field emission triode. (c) Field emission current density versus applied electric field curves under the gate voltages of 0, 10 and 18 V. The inset shows the corresponding Fowler–Nordheim plots.

grown ZnO NWs are $a = b = 3.25$ Å and $c = 5.21$ Å, which are consistent with what is recorded in ICDD No 80-0074. An HR-TEM image and the corresponding selected area electron diffraction (SAED) pattern of the hydrothermally grown ZnO NWs are shown in figure 3(b), illustrating the growth orientation and crystal structure of the NWs. As shown in the figure, the ZnO NWs grew uniformly along the [002] direction and the distance between parallel [002] lattice fringes of the ZnO NW is 5.21 Å. The SAED pattern indexed in figure 3(b) shows that the ZnO nanowire is a single-crystalline structure. The lattice constants calculated from the indexed pattern are $a = b = 3.25$ Å and $c = 5.21$ Å, which are consistent with those calculated from the XRD result.

The emission current density (J) versus gate bias (V_g) characteristic plots at various applied electric fields (E_a) are shown in figure 4(a), indicating that the controllable transistor behaviour can be divided into three parts: gate leakage region, linear region and saturation region. After E_a becomes larger than the threshold electric field, the electrons can emit from ZnO NW emitters without applying V_g. Then, J decreases with increase in V_g in the gate leakage region. With increase of V_g from 0 V, the electric field gradient near the ZnO NW emitters will increase due to the short emitter–gate spacing, and consequently some emitted electrons might be trapped by the gate under the gate leakage region, which results in the lowering of J. The emission current density in the gate leakage region decreases as the gate bias increases since there are more electrons trapped by the gate. As V_g is continuously increased up to 14 V, J abruptly increases in the linear region. The linear intercept on the V_g axis is defined as the threshold gate voltage of the linear region, V_{gth}. It is believed that the induced electric field gradient in the linear region is large

enough to accelerate the electrons; consequently, the emitting electrons gain momentum while passing through the gate to the anode without being trapped. Finally, the field emission current density is saturated when V_g is larger than 18 V. The high emission current of the triode operated in the saturating region may be due to the short gate–tip spacing, small gate aperture and high aspect ratio of the ZnO NWs. J saturation in the saturating region occurs owing to the space charge effect of the semiconductor emitters [16]. Here, the gate leakage region is defined as the field emission off region and the saturation region is the on region. Then, the on/off current density ratio of this field emission triode is about 10^2 under the anode electric field of 2.2 V μm^{-1}.

The field emission characteristics can also be observed in the variation of the small single transconductance (g_m). Figure 4(b) depicts the relationships between g_m and V_g for the ZnO NW based field emission triode. g_m is expressed as follows:

$$g_m = \left.\frac{dI_e}{dV_g}\right|_{V_a}. \quad (1)$$

It is to be noted that g_m is nearly zero below V_{gth} because I_e is very small in the gate leakage region. g_m increases in the linear region, goes through a maximum at the point of inflection of the linear region to the saturation region in the J–V_g curve, and then decreases in the saturating region. The ZnO NW based triode exhibits a high g_m of 2.2 μS under the applied electric field of 2.2 V μm^{-1} and a low operating gate bias of 17 V, which is the optimized operation voltage of the field emission triode. μ is another parameter used to evaluate the ability of the gate voltage to respond to the emission current density, depending on the anode voltage (V_a) and the gate voltage (V_g), which is expressed as

$$\mu = \left.\frac{dV_a}{dV_g}\right|_{I}. \quad (2)$$

From figure 4(a), we find that μ is about 100 below the current density of 2 mA cm^{-2}. Although this μ value is smaller than that ($\mu = 250$) for a triode based on a plasma-enhanced chemical vapour deposition diamond film [17], the low temperature (75 °C) synthesized ZnO NWs are used here for the first time in the fabrication of a field emission triode device with controllability.

The relationship between J and E_a for the ZnO NW based triode for different V_g is shown in figure 4(c). The turn-on electric field (E_{on}, at a current density of 1.0 μA cm^{-2}) and threshold electric field (E_{th}, at a current density of 1.0 mA cm^{-2}) are 1.6 and 2.1 V μm^{-1} under zero gate bias, respectively. As the V_g increases to 10 V, J is depressed to 36 μA cm^{-2} under an E_a of 2.2 V μm^{-1}. When V_g increases to 18 V, E_{th} slightly decreases to 2.0 V μm^{-1} but J abruptly increases to 12 mA cm^{-2} under an E_a of 2.2 V μm^{-1}. The corresponding F–N plots ($\ln(J/E^2)$ versus E^{-1}) of the ZnO NW based triode are depicted in the inset of figure 4(c), indicating that the measured field emission characteristics fit the F–N relationship. The F–N relationship is as follows:

$$J = \frac{A\beta^2 E^2}{\phi} \exp\left(\frac{-B\phi^{3/2}}{\beta E}\right) \quad (3)$$

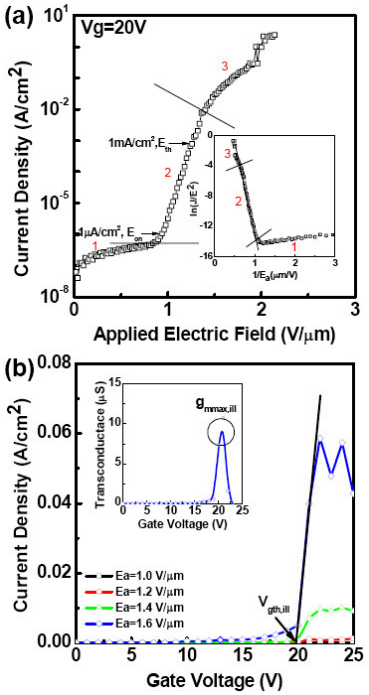

Figure 5. (a) Photo-enhanced field emission characteristics of the ZnO NW triode device operating at a V_g of 20 V. The inset shows the corresponding F–N plots. (b) Photo-enhanced field emission current density versus gate voltage (J–V_g) curves under various applied electric fields; the inset shows g_m versus V_g under an E_a of 2.2 V μm^{-1}.

where J is the current density, E the applied field, Φ the work function of the ZnO (5.37 eV), β the field enhancement factor, $A = 1.56 \times 10^{-10}$ (AV^{-2} eV) and $B = 6.83 \times 10^3$ (V $eV^{-3/2}$ μm^{-1}) [9]. Thus, the value of β can be calculated from the slope of the F–N plot. As shown in the figure, the F–N plot under a V_g of 10 V deviates from the F–N fitting, and those under voltages V_g of 0 and 18 V obey the relationship with the same slope. The calculated β value for a ZnO NW based triode under a V_g of 0 V is 3048. It is well known that the β value depends only on the geometry, structure, tip size and number of emitters on the substrate; thus, the β value should be constant as gate voltage varies. It is suggested that the observed large deviation from the F–N fit under a V_g of 10 V is attributable to the gate trapping being the main mechanism in the gate leakage region.

The measurement of field emission properties of a field emission triode based on low temperature synthesized ZnO NWs under 30 W incandescent lamp irradiation with a V_g of 20 V (operating in the gate controlled saturation region) was carried out to investigate the influence of the illumination on the triode. As shown in figure 5(a), the triode operating in the saturation region exhibits typical field emission characteristics under illumination. This J–E curve can also be divided into three parts: zero emission (region 1 of figure 5(a)), F–N field emission (region 2) and current saturation regions (region 3). E_{on} and E_{th} decrease to 0.9 and 1.3 V μm^{-1}, respectively, and the maximum current density increases to 2.5 A cm^{-2} under the V_g of 20 V and E_a of 2.2 V μm^{-1}. The β value (3050) of the illuminated ZnO NW based field emission triode calculated from the slopes of the F–N plot (see the inset in figure 5(a)) is

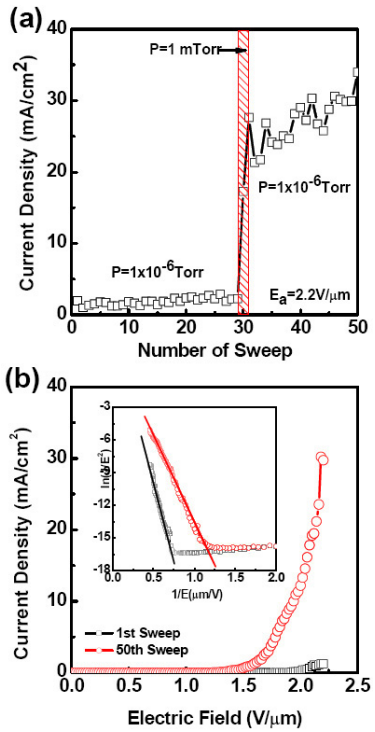

Figure 6. (a) The emission current density of the ZnO NW based field emission triode under various pressures. (b) The 1st and 50th sweeps of J–E_a curves and the corresponding F–N plots. (This figure is in colour only in the electronic version)

close to that of the dark one. Therefore, it is demonstrated that the carriers in the ZnO NWs are excited during the illumination, leading to increase of the emission current density.

The J–V_g plots with various fields E_a for a triode under 30 W incandescent lamp irradiation are shown in figure 5(b). It is indicated that the triode under such illumination keeps the transistor showing controllable behaviour that can be separated into a gate leakage region, linear region and saturation region. There is a large increase in the field emission current density under the optical illumination and the threshold gate bias of the triode operated under the illumination is about 20 V. The average current density in the off region under the field E_a of 2.2 V μm^{-1} is about 0.1 mA cm^{-2}, while that in the on region is about 0.5 A cm^{-2}. Thus, the triode exhibits controllable field emission characteristics under illumination, and the on/off current density ratio of this triode is about 5000 under the anode electric field of 2.2 V μm^{-1}. The inset in figure 5(b) shows the relationship between g_m and V_g with an E_a of 1.6 V μm^{-1} under illumination; this exhibits a high g_m of 10 μS under the anode field of 1.6 V μm^{-1} and a gate bias of 20 V, which is the optimized operation voltage for such a triode. Moreover, the μ value is about 200 under 2 mA cm^{-2}. Obviously, not only was the emission current density photoenhanced but also the controllability is enhanced under the optical illumination.

Figure 6 shows the field emission characteristics of the triode measured under various pressures, obtained to investigate the influence of the measuring pressure on the characteristics. This ZnO NW based triode was swept from 0 to 2.2 V μm^{-1} with a V_g of 0 V (avoiding the effects from the gate) under 1×10^{-6} Torr in the first 29 operations. In the first 29 tests, the field emission current densities are

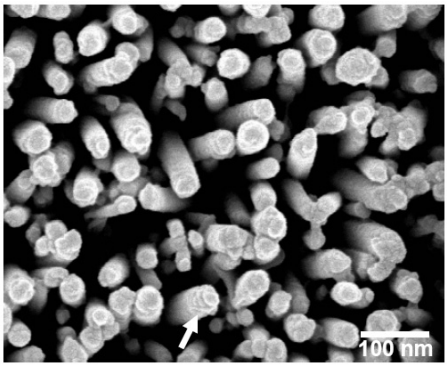

Figure 7. FE-SEM images of ZnO NWs after the 50th J–E_a sweep.

similar to those obtained with the average current density of 2 mA cm^{-2}. Then, the following two sweeps were carried out under 1×10^{-3} Torr with Ar gas flowing in, and the current density is abruptly increased to 27 mA cm^{-2}. Finally, the pressure was decreased to 1×10^{-6} Torr again, for the last 19 operations and the field emission current density remains at the average value of 27 mA cm^{-2}, which shows a significant increase in comparison with that in the first 29 tests under the same measuring pressure. The field emission characteristics of the 1st and 50th sweeps of the triode are depicted in figure 6(b), indicating that the E_{th} of the 1st sweep is 2.1 V μm^{-1} while that of the 50th sweep 1.6 V μm^{-1}. The calculated β value of the 50th sweep of this triode device is 5203. Thus, such a triode exhibits better emission properties, including low turn-on and threshold electric fields, high emission current density and a high β value after the measurement at the high pressure of 1×10^{-3} Torr.

The field emission ability and β value strongly depend upon the morphology of the ZnO NWs. Figure 7 shows the FE-SEM image of the ZnO NWs after measuring in high pressure and sweeping 50 times, indicating that these ZnO NWs have smaller tips than the original ones (figure 2). It is suggested that these ZnO NWs measured under high pressure were bombarded with argon ions leading to the formation of smaller tips at the front of the NWs. Therefore, the observed improved emission properties of the triode are mainly due to such smaller tips of ZnO NWs. Moreover, these ZnO NWs exhibit the better field emission ability and higher β values than ZnO NWs synthesized by the hydrothermal method ($\beta \sim 550$) [18] and ZnO nanoneedles formed by Ar ion bombardment ($\beta \sim 1134$) [19]. This result also provides a possible simple method for enhancing the field emission properties of ZnO NW based triodes.

On the basis of the previous studies by our group [9], we can say that vapour–liquid–solid (VLS) synthesized ZnO NWs with a higher aspect ratio and smaller tip diameter exhibit better field emission characteristics (low threshold electric field, high current density and high β value ($\beta \sim 7180$)). However, the ZnO NWs used in field emission devices are restricted to ones having high reaction temperatures. In this paper, the hydrothermal method provides a low temperature process for fabricating ZnO NWs, which would be not only compatible with the Si based microelectronic fabrication process but also possible for use in polymer based flexible electro-optical applications.

4. Conclusions

In this report, a field emission triode based on low temperature hydrothermally grown ZnO NWs was fabricated and characterized. The ZnO NW based triode emitter was designed with a 100 × 100 μm^2 cathode active region, which exhibits gate controllable behaviour and emits electrons at a threshold gate bias of 14 V with the saturation current density of 12 mA cm^{-2} and g_m of 2.2 μS, at a low operating E_a of 2.2 V μm^{-1} and an on–off ratio of up to 10^2. These controllable field emission properties of the triode can be enhanced by illumination. Moreover, the ZnO NW based triode exhibited better field emission properties when it was measured under high pressure, leading to the formation of smaller tips of the ZnO NWs. Our field emission triode with controllable transistor characteristics is expected to be appropriate for field emission display applications.

Acknowledgment

This work was supported by the National Science Council of Republic of China. Contract No NSC 94–2216–E–009–007.

References

[1] Lee C Y, Li S Y, Lin P and Tseng T Y 2005 *J. Nanosci. Nanotechnol.* **5** 1088
[2] Chen Y J, Li Q H, Liang Y X, Wang T H, Zhao Q and Yu D P 2004 *Appl. Phys. Lett.* **85** 5682
[3] Hofmann S, Ducati C, Kleinsorge B and Pobertson J 2003 *Appl. Phys. Lett.* **83** 4661
[4] Lee O J and Lee K H 2002 *Appl. Phys. Lett.* **82** 3770
[5] Zhinov V V, Givarfizov E I and Plekhanov P S 1995 *J. Vac. Sci. Technol.* B **13** 418
[6] Xu C X, Sun X W, Yuen C, Chen B J, Yu S F and Dong Z L 2005 *Appl. Phys. Lett.* **86** 011118
[7] Fujihara S, Suzuki A and Kimura T 2003 *J. Appl. Phys.* **94** 2411
[8] Miyata T, Minamino Y, Ida S and Minami T 2004 *J. Vac. Sci. Technol.* A **22** 1711
[9] Li S Y, Lin P, Lee C Y and Tseng T Y 2004 *J. Appl. Phys.* **95** 3711
[10] Zhang B P, Wakatsuki K, Binh N T, Segawa Y and Usami N 2004 *J. Appl. Phys.* **96** 340
[11] Wu J J and Liu S C 2002 *Adv. Mater.* **14** 215
[12] Li S Y, Lin P, Lee C Y, Ho M S and Tseng T Y 2004 *J. Nanosci. Nanotechnol.* **4** 968
[13] Li Y B, Bando Y and Golgerg D 2004 *Appl. Phys. Lett.* **84** 3603
[14] Tsai C L, Chen C F and Lin C L 2002 *Appl. Phys. Lett.* **80** 1821
[15] Han I T, Kim H J, Park Y J, Lee N, Jang J E, Kim J W, Jung J E and Kim J M 2002 *Appl. Phys. Lett.* **81** 2070
[16] Lu C W and Lee C L 1998 *J. Vac. Sci. Technol.* B **16** 2876
[17] Wisitsora-at A, Kang W P, Dasidson J L, Kerns D V and Fisher T 2003 *J. Vac. Sci. Technol.* B **21** 614
[18] Cui J B, Daphlian C P, Gibson U J, Püsche R, Geithner P and Ley L 2005 *J. Appl. Phys.* **97** 044315
[19] Yang H Y, Lau S P, Yu S F, Huang L, Tanemura M, Tanaka J, Okito T and Hng H H 2005 *Nanotechnology* **16** 1300